A FINITE ELEMENT STUDY OF DECK SHRINKAGE AND STRESS ANALYSIS IN COMPOSITE BRIDGE GIRDER SYSTEMS

Tiffany R. Cartier, EIT, Bridge Engineer, URS Corporation, Rocky Hill, CT
Brian D. Swartz, PE, Dept. of Civil Engineering, University of Hartford, CT

ABSTRACT

This research uses finite element analysis (FEA) to study the behavior of a precast concrete bridge girder made composite with a cast-in-place deck. Two timely issues related to precast concrete bridge design are investigated:

1. Differential deck shrinkage and its impact on concrete stresses.
2. The use of gross section properties and transformed section properties to compute concrete and steel stresses.

First, the finite element models were developed and validated. Validation is based primarily on comparison with traditional cross-sectional analysis techniques including time step and strain compatibility methods. A rectangular beam section with straight tendons was selected for the analysis.

Upon validation, a comparison of the FEA results and the American Association of State Highway Transportation Officials Load Resistance Factored Design (AASHTO LRFD) Bridge Design Specifications was performed with respect to deck shrinkage. The FEA results were also compared to cross-sectional analyses using gross section properties and another using transformed section properties.

The results of these comparisons support the method for computing the effects of deck shrinkage and the correlation of prestress loss and concrete stress proposed by Al-Omaish et al. Furthermore, numerical results indicate that a significant portion of the deck shrinkage effect is reduced by simultaneous girder creep and that the impact of deck cracking on stresses due to differential shrinkage is minimal.

Keywords: Precast, Prestress, Shrinkage,

INTRODUCTION

The design of prestressed concrete, specifically determining the required initial prestressing force, is typically controlled by service limit checks of stress in the concrete extreme fibers. Prestressing is provided to ensure that all locations in the cross section fall within a strict range of stresses. Very little, if any, tension stress is permitted depending on the application. When stress limits are satisfied, uncracked and nearly elastic response of the concrete follows. Calculation of stresses through the life of the girder requires a sound understanding of the time-dependent effects, specifically creep, shrinkage and elastic stiffening, of the concrete. The analysis is further complicated because the interaction of the concrete and reinforcing steel must be considered.

The time-dependent analysis is traditionally done via an estimate of prestress losses. Knowledge of precast, prestressed concrete construction is essential to understanding the equations involved, so it will be reviewed here briefly. An initial strain (i.e. tension stress) is applied to the steel by hydraulic jacking prior to concrete placement. As the concrete hardens, it bonds to the embedded steel. After the concrete reaches sufficient strength, the strands are cut away from the jacking mechanism such that the concrete maintains the tension strain in the steel. Once transfer has occurred, the steel-concrete system is self-equilibrating. The tension force in the steel creates a compression force in the concrete of equal magnitude. The concrete responds, elastically, to this compression force and shortens. When the concrete shortens, the bonded steel also shortens and loses some of its initial stress. This phenomenon is frequently termed “elastic shortening” loss. As time passes, the concrete shrinks and creeps, continuing to lose volume and allowing the bonded steel to shorten and lose some of its initial stress. The loss of prestress due to these effects can be mostly determined by Hooke’s Law, considering the change in strain of the concrete and the elastic properties of the steel. Furthermore, the steel loses a small amount of stress without a change in strain due to a phenomenon called “relaxation.” Additionally, the concrete strengthens, changing its elastic response characteristics (i.e. elastic modulus), over time. True determination of the prestressing force is complicated by interaction between the steel and concrete, which have very different time-dependent properties.

The effective prestressing force (initial prestressing force less the prestress loss) is traditionally used to determine the stress in the concrete through a combined stress formulation. This approach is convenient, and reasonably accurate. It uses a prestress loss calculation as the means to calculate the change in concrete stress, which is typically the end goal. There are several shortcomings, however, because it is very difficult to separate elastic (strains that do lead to stress) and inelastic (strains that do not lead to stress) effects in the concrete. Therefore the true stress in the concrete (and more importantly its nearness to cracking) is difficult to determine from the effective prestressing force, alone.

Historically these simplifications have not been a major concern because the prestress loss calculations were sufficiently conservative (meaning that loss of prestress was over-predicted) that the amount of prestressing force provided initially was more than sufficient to

counteract future dead load and live load stresses even after considering time-dependent effects.

In recent years there the industry has moved towards refined stress calculations and move towards more rigorous and precise methods. The National Cooperative Highway Research Program (NCHRP) Report 496[1] was the biggest step in this direction. That report, while aiming primarily to extend the scope of prestress loss calculations to better represent the behavior of high-strength concrete girders, also introduced a fundamentally more advanced approach to prestress loss calculations, in general. The method was adopted in the American Association of State Highway Transportation Officials Load Resistance Factored Design (AASHTO LRFD) Specifications[2] and proved substantially more complex than its predecessor. At the charge of the Portland Cement Association, Swartz, Schokker and Scanlon[3] proposed a simplified approach to prestress loss calculations that aimed to maintain a similar level of accuracy. At the time of this writing that proposal, termed the "Direct Method" sits as a Working Agenda Item before the AASHTO T-10 committee.

A few items, in particular, have been raised as concerns through the iterations on this topic in the past several years, and they are the primary subjects of this study. First, the method introduced by NCHRP Report 496 was the first to explicitly consider the composite relationship between a precast girder and a cast-in-place (CIP) deck, particularly the shrinkage restraint afforded by the girder against the deck. Part of the confusion arises from an unfortunate choice of words in the Specification, which characterizes the effect of deck shrinkage as an elastic prestress gain. That approach is theoretically correct, but practically flawed as those applying the traditional approach to stress calculations are accustomed to first determining the effective prestressing force and calculating the concrete stress from there. In other words, this was the first time that the concrete stress calculation and the estimate of effective prestressing force became partially decoupled. Furthermore, many have questioned whether the effect of deck shrinkage is nearly as significant as the AASHTO Specification implies once creep and cracking of the concrete is properly considered in conjunction with the deck shrinkage.

Secondly, the NCHRP Report 496 method was the first to strongly endorse the use of transformed section properties (in which the bonded steel is represented by an equivalent area of concrete in the section property calculations) for calculation of stresses. While there is little argument that the use of transformed section properties is theoretically superior to gross section properties (in which the bonded steel is thought to be concrete, without regard for the vastly different stiffness characteristics, in the section property calculations), the results are thought to be close enough that the additional effort and complication is not warranted. In fact, it seems that the biggest problem has been improper application of transformed section properties, which leads to much larger errors than would the simplification of gross section properties.

This paper documents a study that provides guidance on these issues through a detailed finite element analysis. The analysis considers the interaction of concrete and steel, the interaction between the girder and the deck, and the time-dependent nature of the materials involved. A

finite element study has been chosen in order to discretely separate elastic and inelastic effects so that concrete stresses can be explicitly known and are not dependent upon a prestress loss calculation. The study evaluates the appropriateness of the NCHRP Report 496 approach for time-dependent analysis of prestressed girders. Furthermore, the finite element study validates the use of a detailed time-stepping cross sectional analysis as a benchmark procedure for comparing other methods.

PROBLEM STATEMENT

The research presented in this paper uses finite element analysis (FEA) to study the behavior of a precast concrete bridge girder made composite with a CIP deck. A 30 foot long simply supported girder having a rectangular cross section and straight tendons was selected for the study. Both three dimensional and two dimensional models were developed.

Two timely issues related to precast concrete bridge design were investigated:

3. Differential deck shrinkage and its impact on the concrete stresses.
    - Can deck shrinkage be modeled as an equivalent force?
    - If so, how are girder and deck stresses calculated from that force?
    - By how much is that force reduced when creep is considered?
    - By how much is that force reduced when deck cracking is considered?

4. The use of gross section properties and transformed section properties to compute concrete and steel stresses.
    - How should concrete stresses be determined?
    - How should prestress loss values be interpreted?

METHOD

Investigation of issues related to differential deck shrinkage and the use of transformed section properties was conducted with nonlinear, transient FEA of a three dimensional precast girder with a CIP deck. The model geometry, element assignments, and material properties were selected to most closely represent reality, especially with respect to the time dependent behavior of concrete, with an eye towards computational simplicity, as well. Loading attributes and analysis sequencing were assigned to mimic typical precast concrete bridge construction staging.

Hierarchal analysis techniques were used to validate all finite element model (FEM) geometry, element, material, and loading assignments. Validation is based primarily on comparison with traditional cross-sectional analysis techniques including time step and strain compatibility methods.[3]

Upon validation of the FEM attributes, a series of analyses were created to isolate stress and strain components associated with initial prestress, beam shrinkage, deck placement, differential deck-girder shrinkage, creep, and live load. Stresses from each of the analyses were sampled at the extreme deck concrete fibers, extreme girder fibers, and the prestressing steel centroid.

A two dimensional model of the same structural system was analyzed in tandem with the three dimensional model. Comparison of the analyses results indicated that a two dimensional model could be used to address most the of the research objectives. With this in mind, deck cracking was incorporated only in a two dimensional model. The same procedure for sampling data and isolating stress/strain components was followed for the cracked deck model.

A comparison of the FEA results and the AASHTO LRFD Bridge Design Specifications was performed to examine AASHTO's treatment of deck shrinkage. The FEA results are also compared to cross-sectional analyses using both gross section properties and transformed section properties. Design recommendations are provided based on the results of these comparisons.

DEVELOPMENT OF THE FINITE ELEMENT MODEL

GEOMETRY AND ELEMENT SELECTION

A three dimensional model of a rectangular prestressed concrete beam with a CIP deck was developed and analyzed in Lusas FEA software. The beam contains 12 straight, seven wire prestressing tendons with a strand pattern center of gravity located 14.5 inches from the top of the beam. The theoretical geometry is shown in Figure 1.

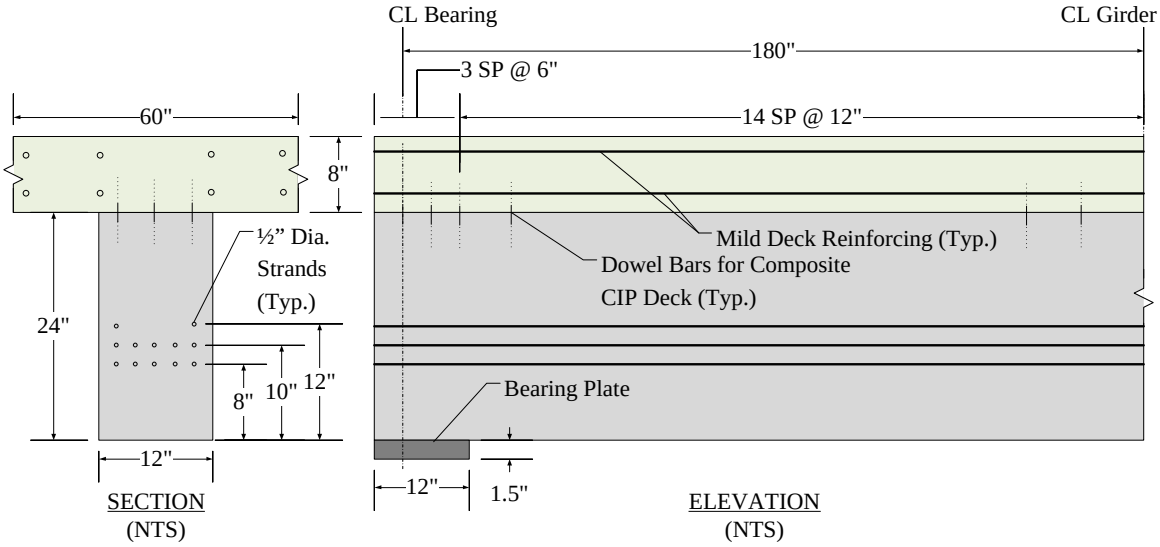

Figure 1. Theoretical geometry of selected prestressed concrete girder with composite CIP deck

The FEM concrete beam and deck geometries are comprised of a series of merged volumes measuring 12 inches in length. The merged volumes provide nodes spaced 12 inches apart along the length of the beam that are used to develop connectivity between the beam and the deck. Hexahedral solid continuum elements (HX20) are assigned to the concrete volumes. The hexahedral elements have a total of 20 corner and mid-side nodes, and are capable of developing stresses and strains in six directions. Interpolation of stresses and strains across elements is quadratic.[4]

The steel tendons and deck reinforcing geometry are also modeled with volumes. Each volume has a rectangular cross sectional area equal to the corresponding circular bar cross section. Using a rectangular cross section simplifies the mesh pattern without introducing global error. To further simplify the model geometry and reduce computational time, the twelve prestressing strands are lumped into one volume located at the strand pattern center of gravity. Although a model with one lumped tendon may exhibit local stresses inconsistent with the actual beam, the extreme fiber stresses are not affected. The same hexahedral solid continuum elements are assigned to the volumes representing steel reinforcing and tendons.

The beam is simply-supported by a steel bearing plate measuring 1.5 in x 12 in x 12 in. While such support is not required for accuracy of midspan stresses and strains, the bearing plate is included for increased representation of reality.

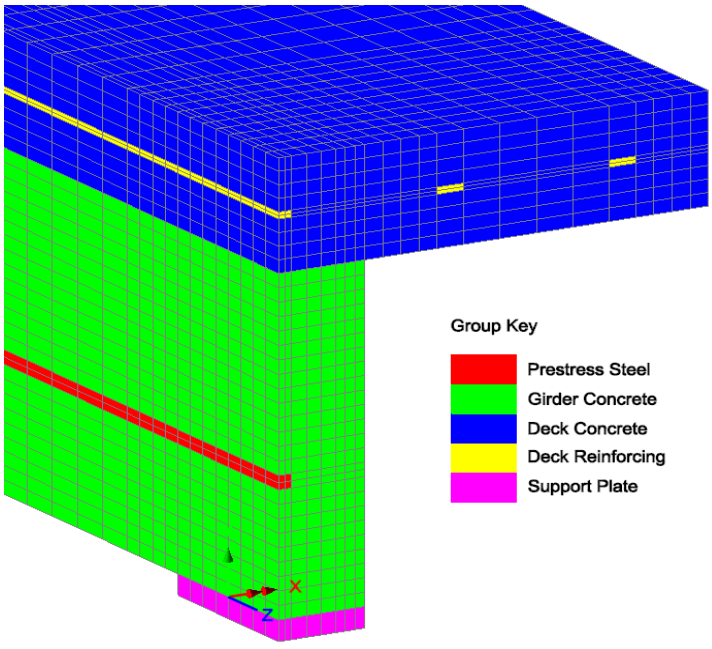

Figure 2. Simplified girder and deck geometry selected for three dimensional FEA

MESH CONTROL

The solid volume mesh is controlled by specifying the number of mesh divisions or element lengths to be generated along lines defining geometric volumes. All elements in the mesh pattern are regular, orthogonal volumes.

Figure 3 shows the dimensions of the mesh pattern assigned to the girder and deck. Lines along the vertical axis of the beam and deck are generally assigned one inch element lengths. Vertical lines defining steel volumes are assigned two mesh divisions to provide a node coincident with the prestressing centroid. An element length of one inch would result in one mesh division through the steel, which is insufficient to obtain accurate stress values. Lines along the transverse axis are also assigned element lengths of approximately one inch. Deck volumes not directly above the girder have a coarser mesh because stresses and strains are not sampled in this region. Element length along the longitudinal axis is mostly controlled by the cross section mesh density. In order to maintain a reasonable element aspect ratio, the longitudinal element lengths should be limited to approximately five inches. A slightly finer mesh is preferred to limit interpolation at the deck connection points. With consideration of these issues, three inch element lengths are assigned to longitudinal lines. Within 24 inches of midspan, the element length is reduced to one inch to further increase accuracy where stresses and strains are sampled.

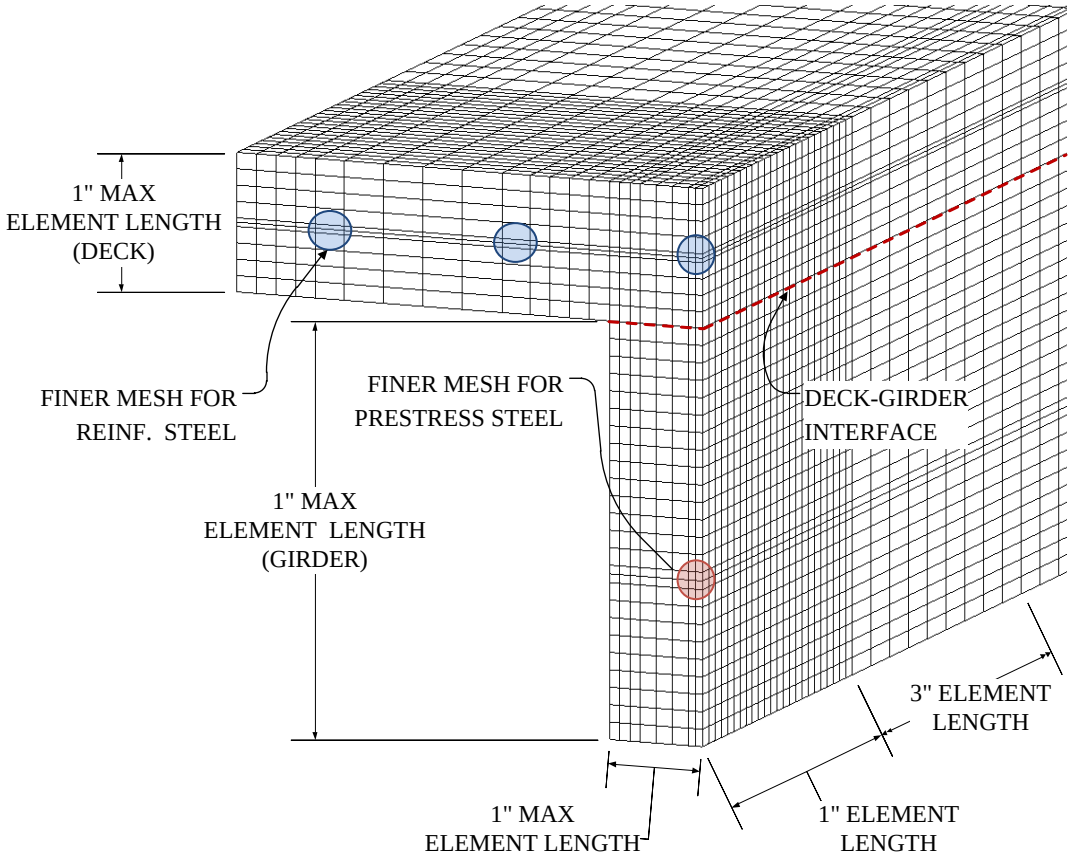

Figure 3. Mesh control assignments

CONSTITUITIVE PROPERTIES

A specialized, built-in constitutive model within Lusas for concrete based on the CEB-FIP Model Code 90[5] is assigned to deck and beam concrete elements. This material is capable of modeling creep and shrinkage behavior of concrete in accordance with the CEB-FIP Model Code, an acceptable analysis method listed in the AASHTO LRFD Bridge Design Manual. The material also compensates for the strength/stiffness gain of concrete over time by incrementing the Elastic Modulus. The parameters used to define the deck and beam CEB materials are provided in Table 1.

Table 1. CEB concrete material properties assigned to the girder and deck

Attribute	Girder Concrete	Deck Concrete
General Material	CEB-FIP	CEB-FIP
Mean Compressive Strength at 28 Days (f_{cm})	8 ksi	5.16 ksi
Modulus of Elasticity at 28 Days (E)	5512 ksi	4763 ksi
Nominal Size (2A/P)	8	7
Density	0.2226E-6 kslinch	0.2226E-6 kslinch
Cement Type	Normal or Rapid Hardening	Normal or Rapid Hardening
Poisson's Ratio (μ)	-	-
Relative Humidity (RH)	70%	70%
Age	28 Days	28 Days

The Lusas age attribute is the equivalent of t_o in AASHTO, which represents the concrete age at initial load application. This attribute is used in conjunction with CEB creep and shrinkage material assignments. An age of 28 days is assigned to concrete in the FEM to produce CEB creep calculations that relate linearly to elastic strain, similar to the AASHTO creep methodology.[6] This also facilitated verification of the CEB material model with hand calculations. Furthermore, the CEB model predicts much higher creep strains than AASHTO. By using an artificially "older" concrete the CEB creep estimates more closely match AASHTO.

Isotropic linear elastic materials are assigned to the deck reinforcing, prestressing tendons, and the bearing plate. Inelastic behaviors of the prestressing tendons such as yield and relaxation are not predicted with the assigned material model. It is reasonable to assume perfectly linear behavior because the steel stresses are within the actual elastic range throughout the staged construction analysis. This assumption is also consistent with AASHTO service design requirements. Relaxation of the prestressing tendons causes a small amount of prestress loss; however, this value is typically assumed constant and is not the focus of this research. Since the advent of low-relaxation steel tendons, losses due to relaxation have become substantially smaller than those due to other contributors. In this research the effects of concrete creep and shrinkage are isolated and the addition of small relaxation effects would only complicate that effort. Material properties input for the reinforcing and tendon steels are provided in Table 2.

Table 2. Steel material properties

	Material	Modulus of Elasticity	Poisson's Ratio
Prestressing Tendon	Isotropic, Elastic	28.5E6 ksi	0.3
Mild Reinforcing & Bearing Plate	Isotropic, Elastic	29.0E6 ksi	0.3

The structural response predicted by FEA must satisfy strain-displacement relations and kinematic assumptions, constitutive relations, and boundary conditions. To meet this requirement, the FEA must account for interaction between the bonded steel and concrete materials. Strain compatibility requires that the steel and concrete have equal strain at tendon locations. Because of the large ratio of steel to concrete stiffness, the prestress tendons effectively restrain the concrete against creep and shrinkage. It is important to note that this restraint, represented by the transformed section coefficients, K_{id} and K_{df}, in AASHTO is inherently included in the FEA prestress loss values and associated concrete stress.

BOUNDARY CONDITIONS

Axisymmetry is applied to reduce computational time associated with three dimensional models. The geometry and loading conditions are symmetric about the longitudinal beam centerline and the transverse section at midspan. The axisymmetric solid model with quarter symmetry is shown in Figure 4. Surfaces along the longitudinal plane of symmetry are fixed in the X directions. Surfaces along the transverse plane of symmetry are fixed in the Z direction. The end of the beam is modeled as a pinned connection by fixing the steel support plate against translation in the Y direction.

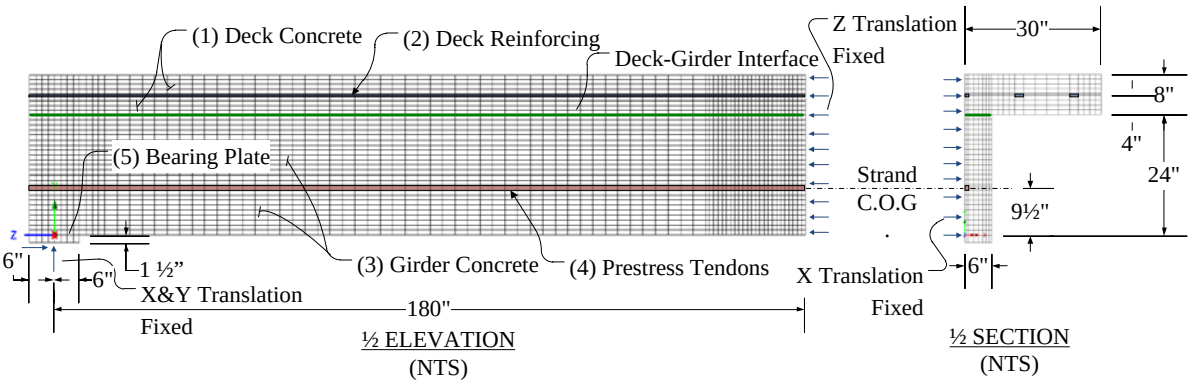

Figure 4. Axisymmetric model with boundary conditions

CONNECTIVITY

Element connectivity is controlled by the merge status of coincident points, lines, and surfaces. The steel prestress tendons are bonded to the concrete by merging the coincident surfaces defining concrete and steel volume boundaries. Similarly, the volumes of beam concrete are connected by merging coincident surfaces, thus allowing a series of adjacent volumes to behave as a single concrete beam. Deck reinforcing and concrete volumes are merged in a similar manner. Unless assigned an unmergable status, Lusas automatically merges coincident geometry.

Connectivity between the precast beam and the CIP deck is defined to closely parallel reality without complicating the FEM. To do this, deck and girder connection is limited to points along the span spaced twelve inches apart. This is accomplished by (1) building the deck geometry separate from the beam geometry, (2) defining merge status of points, lines, and surfaces along the beam-deck interface, and (3) lowering the deck geometry onto the top of the beam. This sequence is depicted in Figure 5. Surfaces, longitudinal lines, and transverse lines along the beam-deck interface are assigned an unmergeable status. Points located along the beam centerline and along a longitudinal line offset four inches from the centerline have a mergeable status. The corresponding points on the bottom of the deck are also mergeable. Upon lowering the deck geometry onto the beam, coincident points with a mergeable status are merged to create the beam-deck connectivity. The merged points behave as infinitely stiff connections between the deck and beam occurring every 12 inches suitably representing shear studs or embedded reinforcement dowels between the girder and deck.

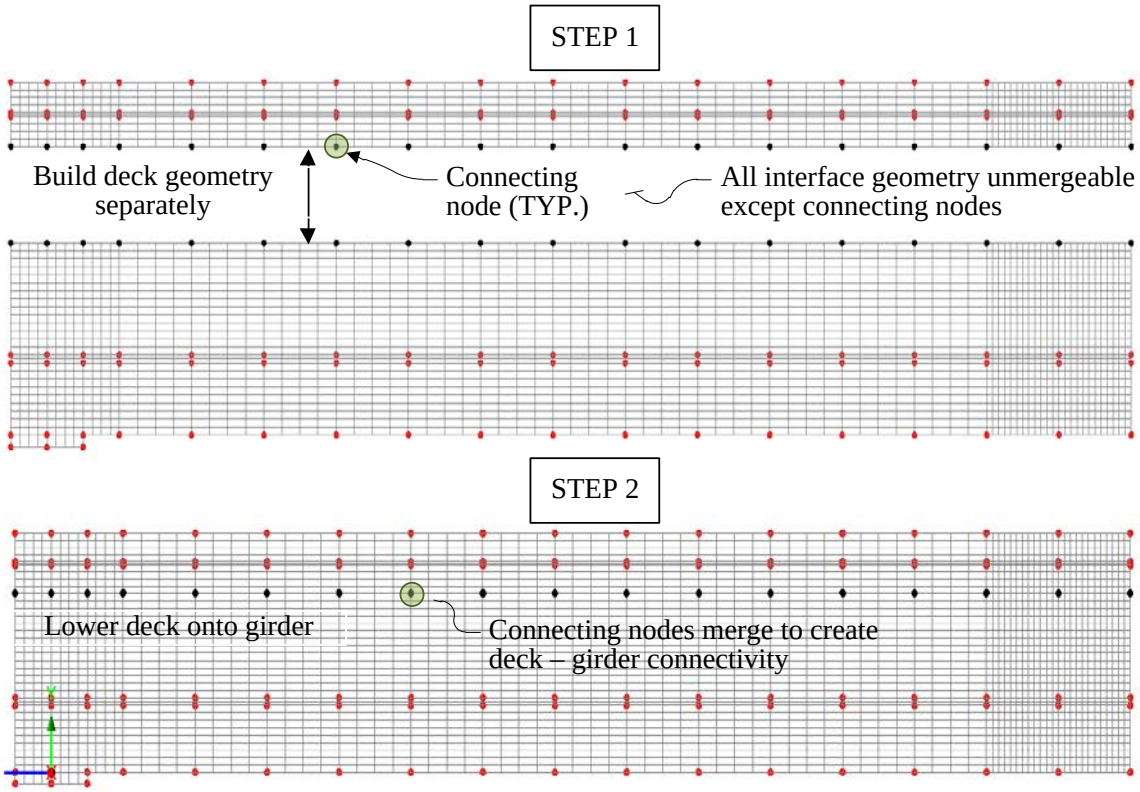

Figure 5. Modeling sequence employed to establish deck-girder connectivity

ACTIVATION/DEACTIVATION

Activation and deactivation options are utilized to model staged construction of the precast beam and the CIP deck. The concrete deck and steel reinforcing volumes are deactivated in the first load case and activated immediately after application of the fluid deck weight, which corresponds to day 90 of the construction sequence. Any loads applied prior to deck activation are resisted by the non-composite section.

CRACKED DECK MODEL

The constitutive properties utilized in the finite element model allow for accurate analysis of the structure under loading conditions within the elastic range of steel and concrete materials. Elastic behavior of the beam concrete, prestressing steel, and deck reinforcing is assumed, consistent with AASHTO design requirements for all construction staging and service load cases. However, the stress range in the deck concrete cannot be assumed linear elastic. Field observations and time step analysis techniques indicate that the deck may exhibit nonlinear behavior in the form of cracking. The results of approximate time step analyses confirm the possibility of nonlinear behavior. Tensile stresses in the deck, which may exceed the rupture stress, develop in the deck due to shrinkage.

To account for potential nonlinearity of the deck concrete, the FEM must be capable of identifying crack formation and analyzing cracked material. As discussed in the *Constitutive Properties* section, the CEB-FIP material, which does not model cracking, is used in order to analyze creep in accordance with AASHTO accepted methods. Due to the inability to model creep, shrinkage, and crack damage with a single material attribute, a physical crack (i.e. gap) is introduced in the deck geometry.

Cracks are defined in the FEM by unmerging points, lines, and surfaces between adjacent volumes of deck concrete. Points and lines along crack locations are also unmerged from the beam. As shown in Figure 6, defined deck cracks are spaced at 48 inches. There are three beam-deck connection locations between each crack.

Deck reinforcing bars are included in the finite element model for the purpose of transferring stress across cracks in the deck. Models with an uncracked deck also contain mild reinforcing to maintain consistent deck and girder geometry. The assigned area of the mild deck reinforcing is somewhat arbitrary because the constitutive properties are completely elastic. Stresses in the reinforcing will increase infinitely without yielding in the FEM regardless of bar size. Furthermore, deck stresses are low (less than 0.5 ksi) during the 360 day construction sequence; therefore, no special attention to deck reinforcing size or total area is required. Bar stresses are sampled only to monitor transfer across deck cracks. Stress transfer is verified by a change from compressive to tensile bar stress occurring in the vicinity of deck cracks. Figure 6 depicts the bar stress contours for the cracked deck model. As expected, a small tensile zone develops at crack locations.

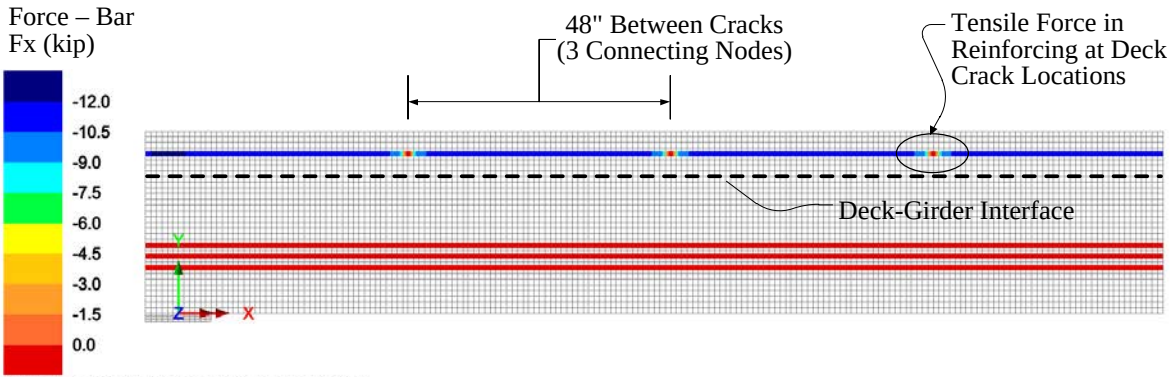

Figure 6. Reinforcing steel force (kip) contours taken from cracked deck model

LOAD CASES

The prestress transfer is modeled with an initial stress in the tendons applied in the first load case on day zero of the analysis. For this model, an initial stress of 202.5 ksi in the longitudinal Z direction is assigned to the lumped tendon.

The self-weight of the precast beam is also applied in the first load case. This accounts for instantaneous cambering of the girder due prestressing transfer. A body force loading attribute, which applies gravitational acceleration to mass, is assigned to the beam concrete volumes.

The weight of the CIP concrete deck, prior to stiffening, is represented with a global distributed load of 0.5 ksf. This load attribute is assigned to the top surface of the beam (one foot width) to produce an equivalent line load of 0.5 klf in order to represent the non-composite beam carrying the weight of the cast-in-place deck. Live load is also represented with a global distributed load having a magnitude 0.2 ksf. This load attribute is assigned to the top surface of the deck (60" wide) to produce an equivalent line load of 1.0 klf. A summary of applied loads is provided in Table 3.

Table 3. Summary of load cases

Applied Load	Load Attribute	Direction	Assigned Value	Assigned Component
Prestress Transfer	Initial Stress	Z	202.5 ksi	Tendon Volumes
Beam Weight	Body Force	Y	Gravity/Unit Weight of Concrete	Girder Volumes
Deck Weight	Distributed	Y	-0.5 ksi	Girder Top Surface
Live Load	Distributed	Y	-0.2 ksi	Deck Top Surface

ANALYSIS CONTROLS

To analyze concrete creep and shrinkage over the 360 day bridge construction, a transient nonlinear analysis is required. The load case controls in Lusas allow the user to specify a nonlinear time domain analysis. For problems involving material nonlinearity, such as creep, a viscous time domain analysis must be selected. The user may then specify time domain parameters such as the initial time step, total response time, maximum increments, and minimum time step. The selected transient analysis controls are listed in Table 4.

Table 4. Time domain parameters assigned to each load case for the 361 Day FEA

Load Case No.	Applied Load	Start Time (Days)	End Time (Days)	Min. Time Step (Days)
Load case 1	Prestress Transfer	1	1	1
Load case 2	Beam Weight	1	1	1
Load case 3	Beam Creep & Shrinkage	1	31	5
Load case 3A	Beam Creep & Shrinkage	31	90	10
Load case 4	Deck Weight	91	91	1
Load case 5	Deck Activation	91	91	1
Load case 6A	Creep & Shrinkage of Composite Section	91	120	5
Load case 6B	Creep & Shrinkage of Composite Section	120	360	10
Load case 7	Live Load	361	361	1

FINITE ELEMENT MODEL VERIFICATION

Verification of the finite element models developed for this research was achieved through a hierarchal analysis. Several test models were analyzed and compared to manual calculations to verify geometry, material, element, loading, and staged construction attributes. The following is a brief description of the verification process.

1. A two dimensional reinforced concrete beam was analyzed. The finite element model response to concentrated loads at third points was compare to hand calculations using gross, net, and transformed section properties.

   The two dimensional reinforced concrete beam model was extended to three dimensions. The finite element model response to concentrated loads at third points was compared to hand calculations using gross, net, and transformed section properties. The following conclusions were drawn from these analyses:

   - The finite element software predicts elastic stresses consistent with cross section analysis using transformed section properties.
   - Reinforcing modeled with structural bar elements does not displace surrounding concrete.
     - Solid continuum elements should be used for three dimensional modeling is a precise representation of realistic cross sectional properties is needed.
     - Two dimensional modeling will exhibit slight error. This error is known and corresponds to the use of transformed section properties that include the displaced area of concrete.

2. A two dimensional model of a prestressed concrete beam was developed. Several trials were conducted using various loading attributes to model prestress transfer. Analysis results from each loading attribute were compared to manual calculations to determine which attribute best represents prestress transfer. In this phase the following items were verified:

   - Initial stress is an acceptable loading attribute for modeling prestress.

3. A two dimensional prestressed beam with a deck activated after transfer and application of self-weight was analyzed. The deck and girder stress outputs were inspected to verify the functionality of deactivation/activation attributes used in modeling staged construction. The following conclusions were drawn from this analysis:

   - Deck weight must be applied prior to deck activation in order for the load to act only on the non-composite section.
   - At activation, deck stresses and strains are zero. In other words, the state of stress in the deck elements is not affected by deformations in the girder that occur prior to deck activation, a true representation of reality.

4. A two dimensional prestressed beam with a shrinking deck was analyzed to confirm stress transfer from the deck to the beam with a focus on the response to differential shrinkage. The concrete and steel stresses developed through the section at various times were compared to time step calculations. The following conclusions were drawn from this analysis:

    - Manual shrinkage strain input as a function of time is an acceptable way to model shrinkage.
    - Stress transfer from the deck to the beam due to differential shrinkage is consistent with stress distributions predicted using equilibrium and strain compatibility analysis methods.

5. A two dimensional CEB concrete (shrinkage option deselected) column with a compressive axial load was analyzed to validate the specialized CEB-FIP material attribute. The FEA creep strain output was compared to manual calculations based on the CEB-FIP code. A second CEB concrete column model without external loads and with the CEB shrinkage option selected was analyzed. Shrinkage strains over time were compared to hand calculations based on the CEB-FIP code. The following determinations were made in this phase:

    - The specialized CEB material creep response is approximately consistent with value calculated manually based on the CEB-FIP code.
    - The assigned age at activation for the concrete must be 28 days to avoid a nonlinear variable modulus of elasticity that cannot be verified with current manual calculations.
    - The specialized CEB material shrinkage strains differed significantly from manually calculated values based on the CEB-FIP code.
    - To overcome differing creep coefficients and shrinkage strains between manual calculations and those observed in Lusas, the shrinkage strains and creep coefficients were extracted from Lusas for use in the time step model verification.

ANALYSIS RESULTS

COMPONENT ISOLATION PROCEDURE

Separation of stress and strain components was achieved through a series of finite element models. A brief description of the modeling sequence used to isolate stresses and strains due to prestress transfer, external loads, girder shrinkage, deck shrinkage, and creep is provided in the numbered list below. Unless otherwise stated, each model has the geometry, steel material properties, loadcases, and analysis controls described in the *Development of the Finite Element Model* section of this report. Deck and girder concrete elastic moduli are 4763 ksi and 5512 ksi, respectively. Stresses and strains were sampled from each model at the prestress centroid and extreme top and bottom fibers of the deck and girder at midspan.

1. Model free shrinkage of mass concrete
   - Deck: Isotropic material with CEB shrinkage (no creep)
   - Girder: Isotropic material with shrinkage (no creep)
   - Two beams of mass concrete with dimensions matching the deck and girder
   - No loads
   - Strains output from this model represent uniform shrinkage in the girder and deck.

2. Model elastic effects due to prestressing and external loads
   - Deck: Isotropic material
   - Girder: Isotropic material
   - Static nonlinear analysis
   - Stress/strain values represent the effects of prestressing and external loading.

3. Model uniform shrinkage of girder
   - Modify the deck shrinkage rate to match the girder shrinkage rate after the time of deck placement
   - Girder: Isotropic material w/CEB shrinkage.
   - Deck: Isotropic material with manual input modified shrinkage strains
   - Effect of Uniform Girder Shrinkage = (3) – (2)

4. Model interactive shrinkage between girder and deck
   - Girder: Isotropic material w/CEB shrinkage
   - Deck: Isotropic material w/CEB shrinkage
   - Differential Shrinkage = (4) – (3)

5. Model Total Effect of Creep, Shrinkage, Prestressing, and External Loads
   - Girder: CEB Material with creep and shrinkage
   - Deck: CEB Material with creep and shrinkage
   - Effect of Girder and Deck Creep = (5) – (4)

Figure 7 shows the components of prestress loss over the 361 day FEA. The six stress components are the results of steps one through five of the isolation procedure described above. Positive stress values correspond to a prestress loss, while negative stress values correspond to a prestress gain. Initial prestressing loss represents the reduction in tension stress due to instantaneous elastic shortening of the concrete girder. The evident gain in prestress due to external loads is the result of an overall tension increment below the girder neutral axis. This should not be interpreted as a gain in concrete pre-compression because the associated bottom fiber concrete stress component is also tensile.

Although deck-girder differential shrinkage is expected to cause a gain in prestress, Figure 7 shows a negligible prestress loss. This is likely a result of a prestress strand configuration with a center of gravity in close proximity to the beam centroid for this simplified geometry. Note that differential shrinkage stress components in the top and bottom girder concrete fibers are meaningful quantities.

Beam shrinkage prestress loss increases over time and appears to be approaching a maximum value. This is expected because beam shortening due shrinkage continues over time, but the rate of shrinkage decreases as the concrete ages.

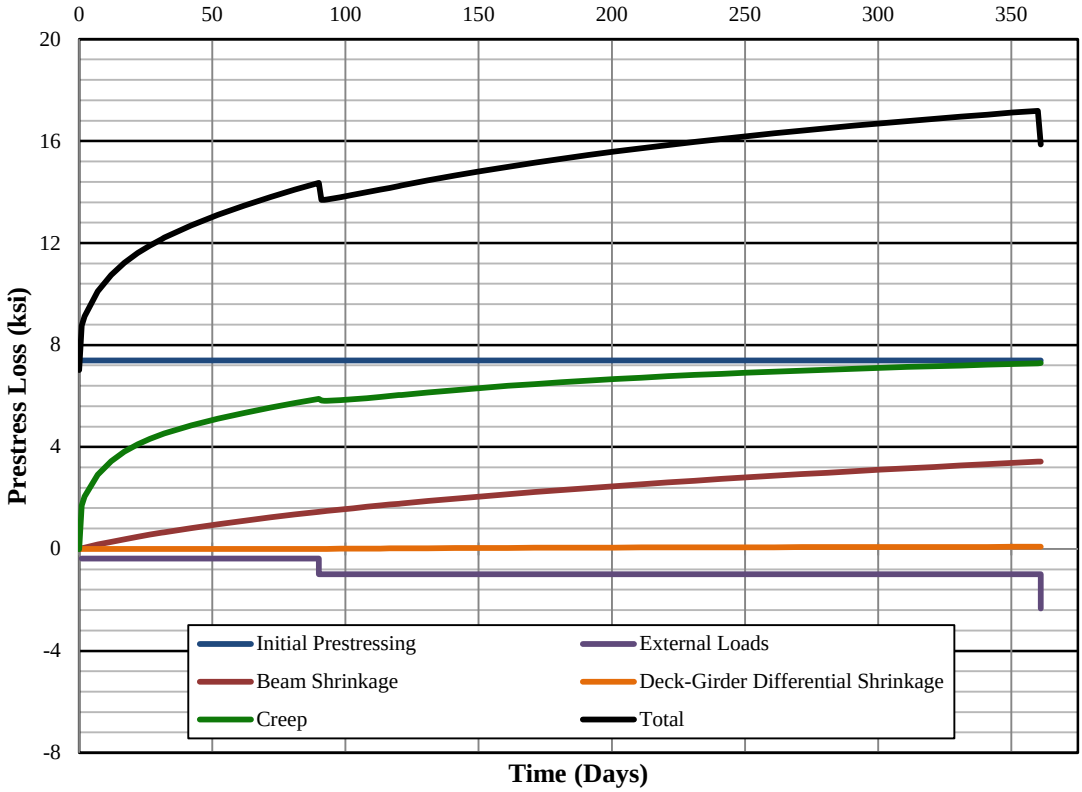

Figure 7. Prestress loss components

Prestress loss associated with creep also increases over time. This is important to remember when considering the effect of creep on the girder bottom fiber stress. As shown in Figure 8, prior to deck placement, creep causes a tensile stress increment in the bottom fiber. This is consistent with the prestress loss due to creep shown in Figure 7, which can be interpreted as a loss in precompression.

After deck placement, creep continues to cause a loss of prestress, but it also causes a simultaneous "softening of differential shrinkage" effect. Because of creep, the bottom fiber is not tensioned by differential shrinkage as much as it might be otherwise. This explains the seemingly compressive creep stress component in the girder bottom fiber after deck placement.

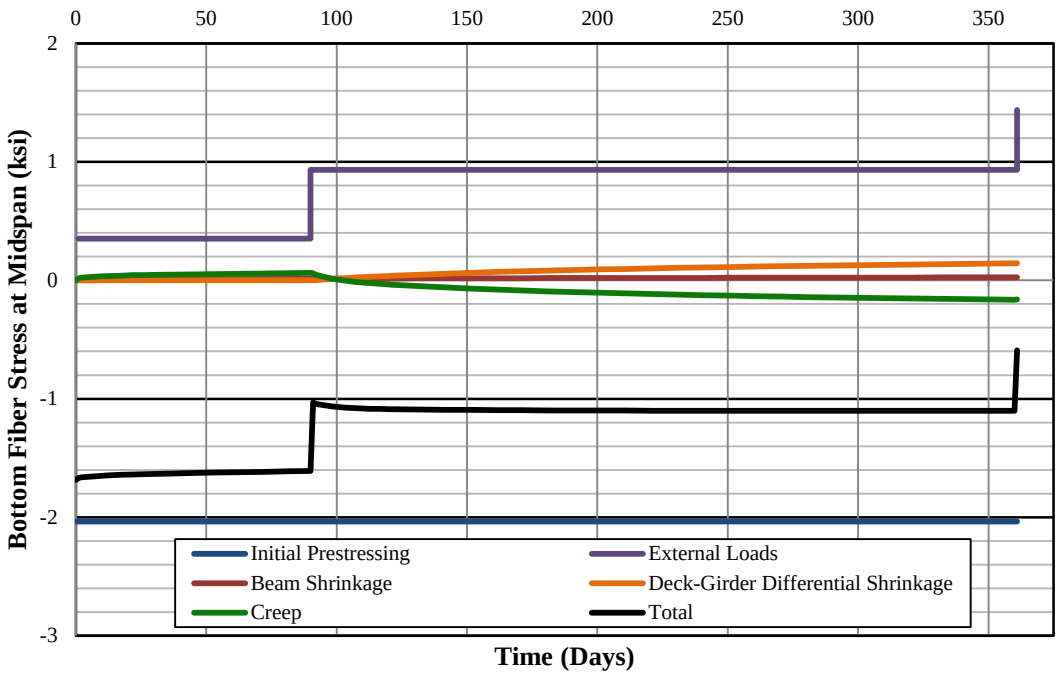

Figure 8. Girder bottom fiber stress components at midspan

Figure 9 shows the components of top fiber stress at midspan over the 361 day FEA. Time dependent effects in the top fiber are negligible until deck placement. Deck weight and differential shrinkage cause compressive stresses in the top fiber. This compression is softened by a tensile stress component associated with creep effects.

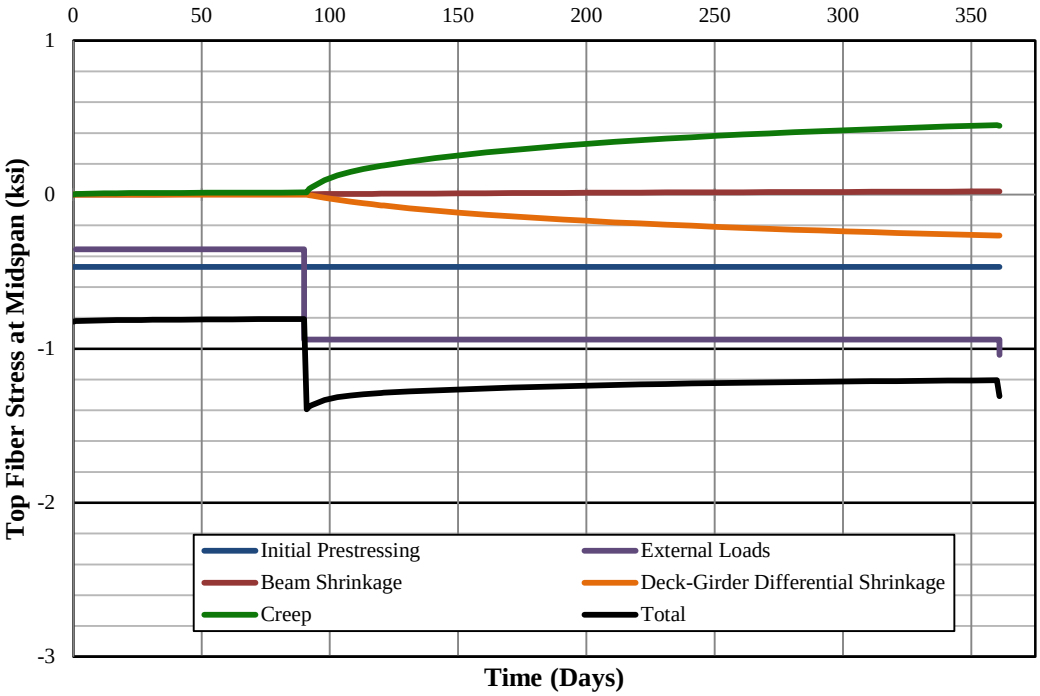

Figure 9. Girder top fiber stress components at midspan

To investigate the effect of creep softening on differential shrinkage, the component isolation procedure continued as described in steps six through eight below.

6. Isolate Effect of **Girder** Creep on Differential Shrinkage
   - Girder: CEB Material with creep and shrinkage
   - Deck: Isotropic material with CEB shrinkage
   - No Loads
   - Effect of Girder Creep = (6) – [(3)-(2)]

7. Isolate Effect of **Deck** Creep on Differential Shrinkage
   - Girder: Isotropic material with CEB shrinkage
   - Deck: CEB Material with creep and shrinkage
   - No Loads
   - Effect of Deck Creep = (7) – [(3)-(2)]

8. Isolate Effect of Simultaneous Girder and Deck Creep on Differential Shrinkage
   - Girder: CEB material with creep and shrinkage
   - Deck: Isotropic Concrete material w/CEB shrinkage
   - No Loads
   - Differential Shrinkage with Girder Creep = (8) – [(3)-(2)]

The four lines shown in Figure 10 represent the results of steps (4), (6), (7), and (8) of the component isolation procedure. Differential shrinkage without creep is as shown in Figure 8 only the scale has been modified to facilitate visual comparison. Differential shrinkage causes a tensile stress increment in the bottom fiber. Figure 10 demonstrates how the magnitude of this tensile stress is reduced by girder and deck creep.

Differential shrinkage causes a compressive stress increment in the top fiber. Figure 11 shows how the magnitude of this compressive stress is reduced by girder and deck creep. Further discussion of creep softening effects on differential shrinkage is provided later in this report.

Detailed descriptions of the models used in component isolation steps (1) through (8) and numerical FEA output are included in Appendices I and II of "A Finite Element Study of Deck Shrinkage and Stress Analysis in Composite Bridge Girder Systems".[7]

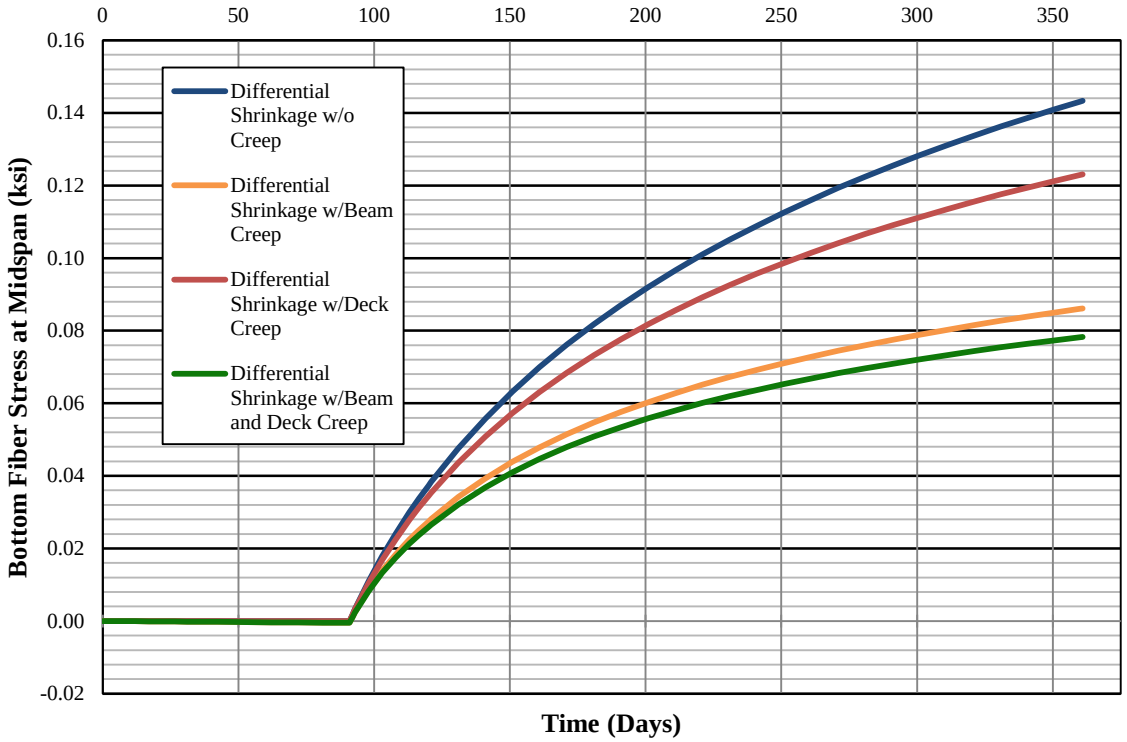

Figure 10. Girder bottom fiber differential shrinkage stress components

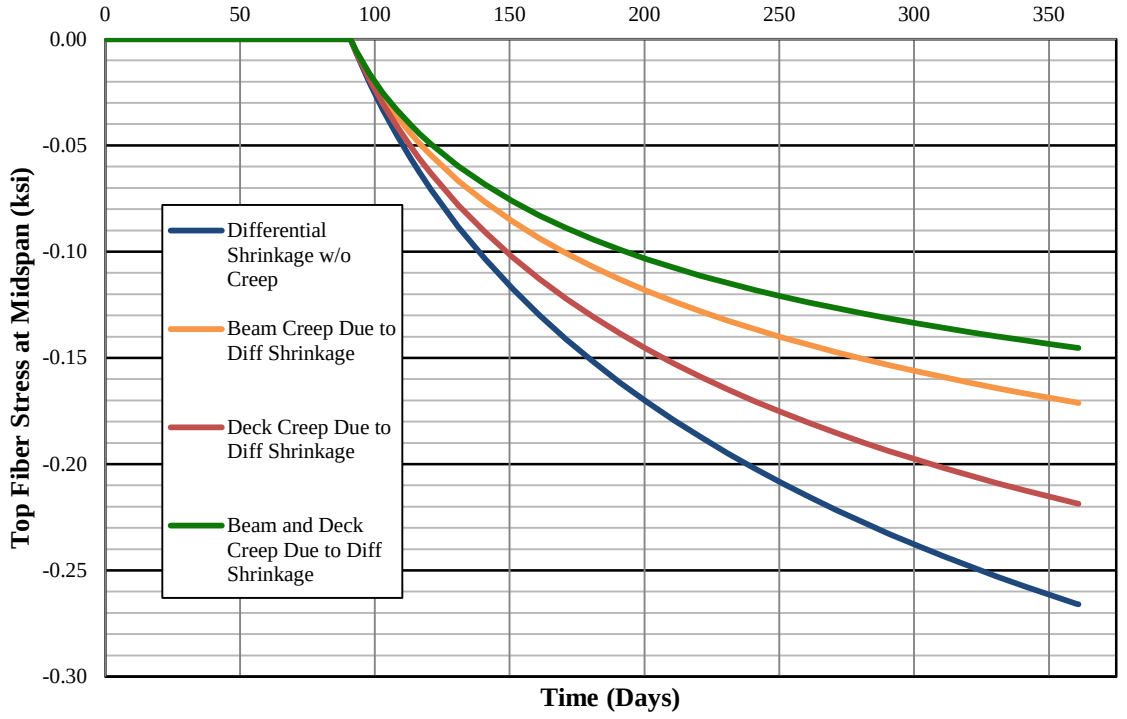

Figure 11. Girder top fiber differential shrinkage stress components

DECK SHRINKAGE

One objective of this research is to investigate the accuracy of current design procedures published in AASHTO that treat deck shrinkage as an external concentrated load positioned on the deck centroid and acting on the gross composite section.[2,8] The Specification instructs designers to compute the change in concrete stress at the centroid of prestressing strands due to the deck shrinkage load using AASHTO Equation 5.9.5.4.3d-2. The computed change in concrete stress is then multiplied by the modular ratio, the beam creep coefficient, and the transformed section coefficient to determine the prestress gain due to deck shrinkage in Equation 5.9.5.4.3d-1. Momentarily neglecting the creep and transformed coefficients, Figure 15 is a representation of the basic mechanics involved in the computation of prestress gain due to deck shrinkage and resulting concrete stresses.

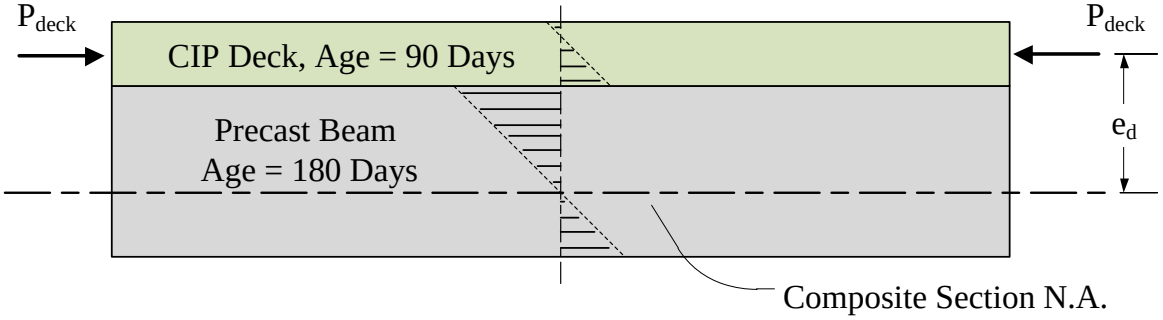

Figure 15. Concept of deck shrinkage as an equivalent force 90 days after deck placement

Deck Shrinkage Modeled as an Equivalent Force

Provisions for computing beam and deck concrete stresses due to differential shrinkage are not explicitly included in AASHTO. A method for calculating extreme bottom fiber stress published in the PCI Journal Article titled *Estimating Prestress Loss in Pretensions, High-Strength Concrete Members* by Al-Omaishi et al. is reproduced below.[6]

$$\Delta f_{cbss} = \left[\frac{-\varepsilon_{ddf} A_d E_{cd}}{1 + 0.7\psi(t_f, t_d)}\right]\left(\frac{1}{A_c} - \frac{y_{bc} e_d}{I_c}\right) K_{df} \quad (1)$$

The accuracy of this approach for computing concrete stresses was investigated by isolating the effects of differential shrinkage using FEA techniques described in the *Component Isolation Procedure* section. To begin, shrinkage of elastic materials described in FEMs (3) and (4) is analyzed. A comparison of Lusas stress outputs and hand calculations based on fundamental mechanics indicates that deck shrinkage can be modeled with an equivalent external force acting at the deck centroid. Having isolated differential shrinkage from the effects of creep and time dependent variation in the concrete Young's modulus, the equivalent force is computed as follows:

$$P_{deck} = (\varepsilon_{ddf} - \varepsilon_{bdf}) E_{cd} A_d \quad (2)$$

If the deck is cast when the beam is 90 days old, ε_{bdf} at 180 days is the difference between the free beam shrinkage strain at 180 days and the free beam shrinkage strain at 90 days. The calculation of P_{deck} built into equation (1) uses the total deck shrinkage strain, resulting in a slight overestimation of concrete stress.

Girder concrete stresses may be computed by applying P_{deck} to the transformed section. A sample calculation of the extreme bottom fiber girder concrete stress is provided.

$$\Delta f_{cbSS} = P_{deck}\left[\frac{1}{A_{tr\_c}} - \frac{y_{bc}e_d}{I_{tr\_c}}\right] \tag{3}$$

The plot shown in Figure 16 demonstrates the resulting error when the same approach is applied to compute deck stresses. The concrete stress component due to differential deck-girder shrinkage 90 days after deck placement (Time = 180 days) is plotted through the composite section. Concrete stresses extracted from the FEA are shown with a solid line. Concrete stresses computed in accordance with proposed equation (3) are represented by a dashed line. Computed girder stresses match FEA results, suggesting that these stresses are accurately predicted by an equivalent point load acting on the transformed composite section. Manually computed deck stresses exhibit a constant error that is shown to equal $\left(\frac{P_{deck}}{A_d}\right)$.

$$P_{deck_{90}} = \left(\varepsilon_{ddf} - \varepsilon_{bdf}\right)E_{cd}A_d = 92.12\ kip \tag{4}$$

$$\frac{P_{deck_{90}}}{A_d} = 0.194\ ksi \tag{5}$$

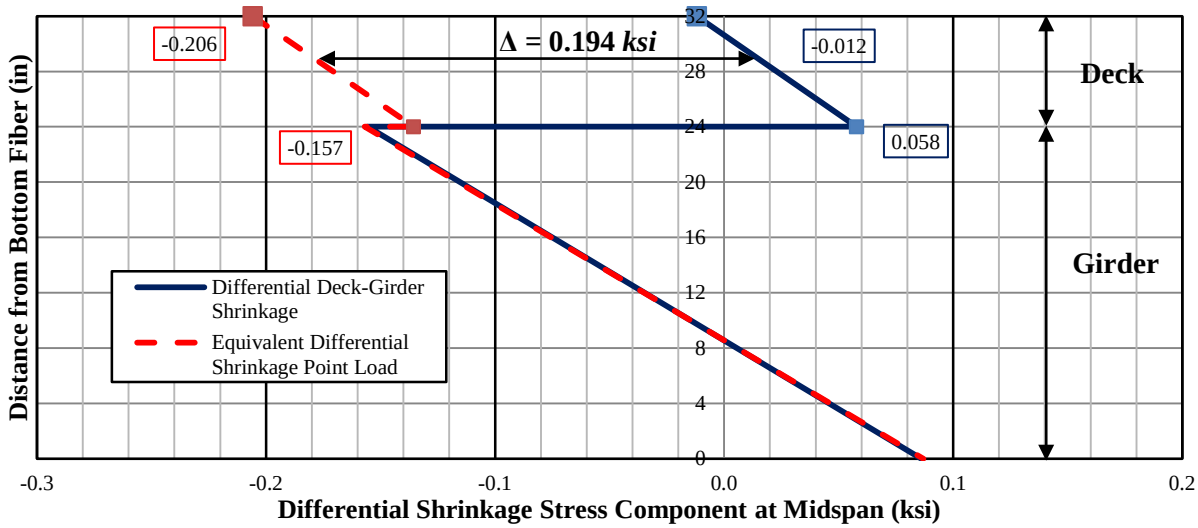

Figure 16. Differential shrinkage stress component plotted through the composite section 90 days after deck placement

In order to maintain equilibrium and strain compatibility at the girder-deck interface, an equal and opposite tensile load must be applied to the deck. The magnitude of the tensile load is that which is required to create a zero net strain in the deck, or $-P_{deck}$. Deck stresses are then computed by adding the axial stress due to the tensile load. The result is shown in equation (5).

$$\Delta f_{cdSS} = P_{deck}\left[\frac{1}{A_{tr\_c}} + \frac{y_{dc}e_d}{I_{tr\_c}} - \frac{1}{A_d}\right] \tag{5}$$

A depiction of how equilibrium and strain compatibility are maintained in the deck is provided in Figure 17.

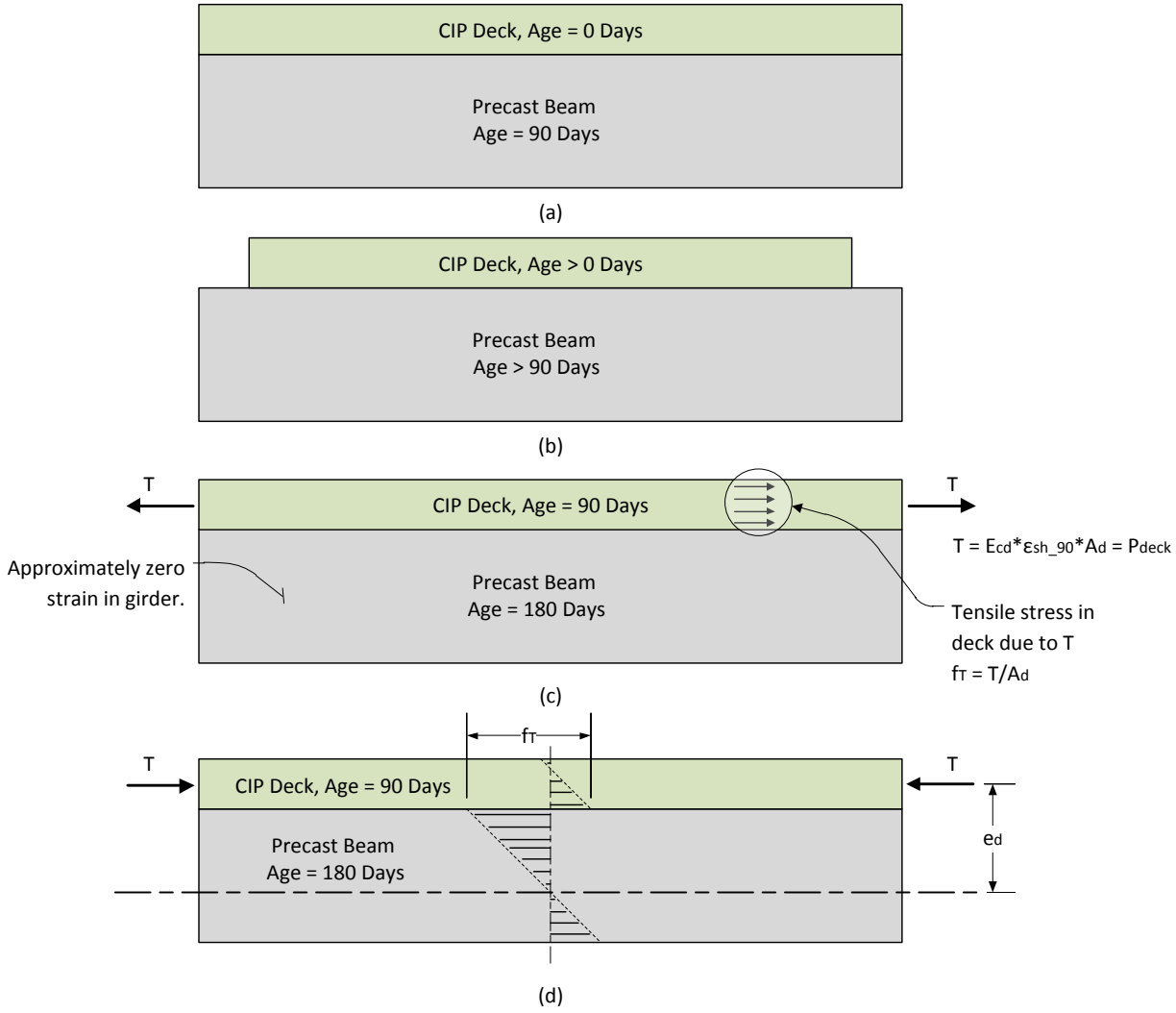

Figure 17. (a) Composite structure at time = 90 days, (b) Free deck shrinkage, momentarily neglecting restraint provided by connection to precast beam, (c) Tensile force, T, needed to re-establish strain compatibility at the deck-girder interface, (d) T reapplied to the composite structure to re-establish equilibrium of the system.

Concrete stresses computed in accordance with equation (5) match FEA output with less than two percent error.

Effect of Creep on Differential Shrinkage

To evaluate the overall effect of differential shrinkage, the analysis is extended to include concrete creep. The concrete stresses induced by differential deck shrinkage are reduced by subsequent creeping of the girder and deck. This reduction in stress may be described as creep softening and is depicted in Figure 18. The plot compares bottom fiber stress due to gross differential shrinkage to differential shrinkage as softened by deck creep, beam creep, and combined deck and beam creep. Data labels are provided at selected times to demonstrate that the portion of net effect of differential shrinkage, which includes beam and deck creep, is approximately 60% of the gross effect, for the geometry and materials used in this model. The same reduction is realized in the extreme top fiber beam concrete.

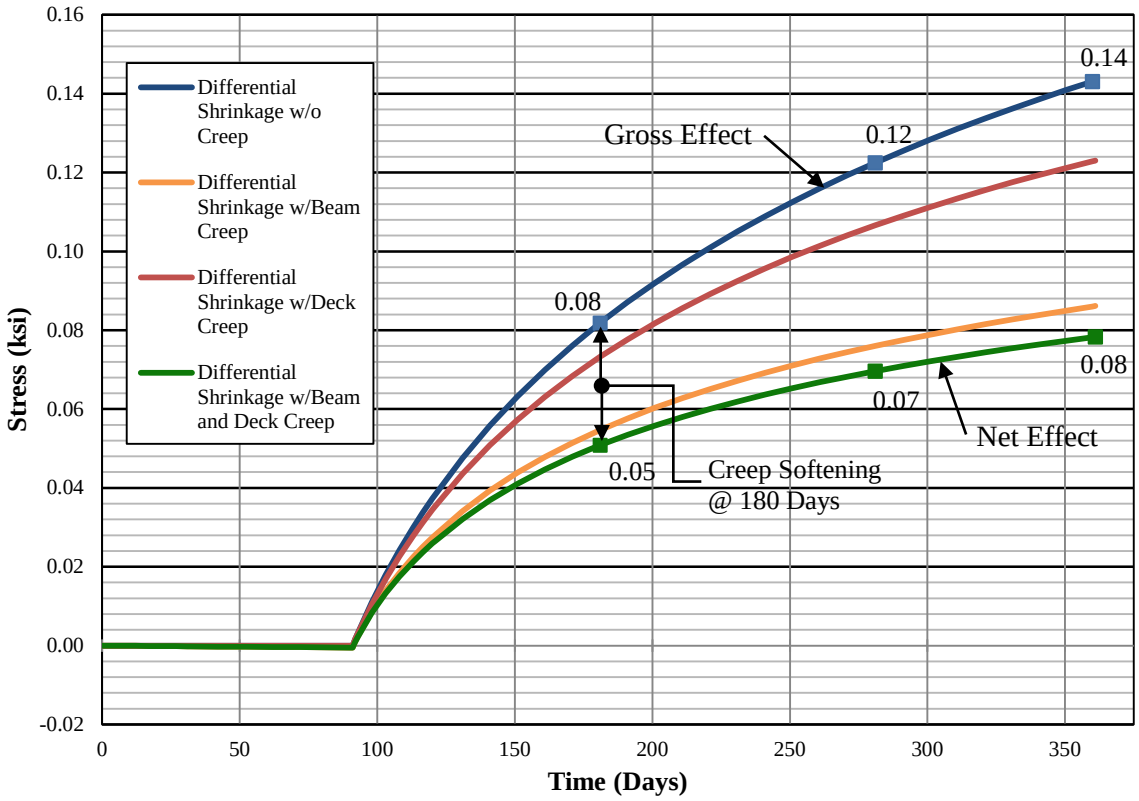

Figure 18. Girder bottom fiber differential shrinkage stress component as softened by creep

Figure 19 shows a snapshot of stress due to differential shrinkage through the composite section 90 days after deck placement (Time = 180 Days). The approximate contributions of isolated deck creep and isolated beam creep are compared to the overall creep softening of differential shrinkage. The compressive stress component in the girder top fiber and the tensile stress component in the bottom fiber are reduced mostly as a result of beam creep.

Similarly, the reduction in deck extreme fiber stresses is largely due to deck creep. It is important to note that differential deck shrinkage causes tension in the bottom of the deck. As a result, deck creep is due to a sustained tensile load. The softening contribution from deck creep shown in Figure 19 is consistent with AASHTO and CEB-FIP codes, which make no distinction between creep due to sustained tensile loads and creep due to sustained compressive loads. Although there may be some discomfort in depending on the deck creep to soften differential shrinkage stresses, its contribution to the total creep is small.

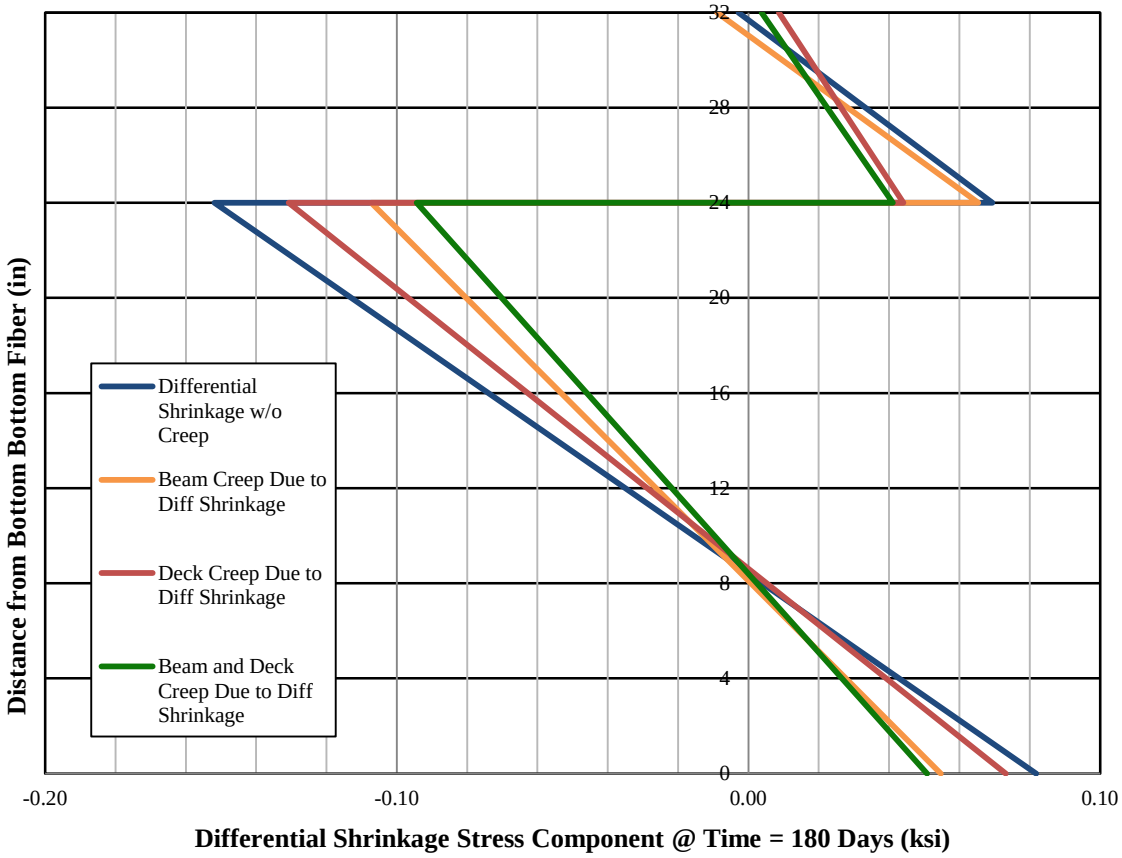

Figure 19. Differential shrinkage concrete stress component as softened by creep plotted through the composite section at Time = 180 days

Effect of Deck Cracking on Differential Shrinkage

Figure 20 compares creep and differential shrinkage bottom fiber stress components extracted from the cracked deck FEM to the original, no crack, results. The dashed lines represent results from the cracked deck analysis, while solid lines depict no crack results. Note that the y axis scale has been exaggerated in order to show some distinction between solid and dashed lines. The y axis scale is restored in Figure 21 to depict the effect of deck cracks on the total bottom fiber stress over time. As shown in both figures, the introduction

of cracks in the deck has little impact on the effects of differential shrinkage. Results of the cracked deck FEA indicate that stress transfer from the deck to the beam, while slightly reduced, will continue provided there is some connection between each volume of deck concrete and the girder and the deck remains uncracked between at least two adjacent transverse shear transfer locations. A comparison of the cracked deck model and the original, no crack, model shows that the effects of differential shrinkage are not softened by the presence of cracks in the deck.

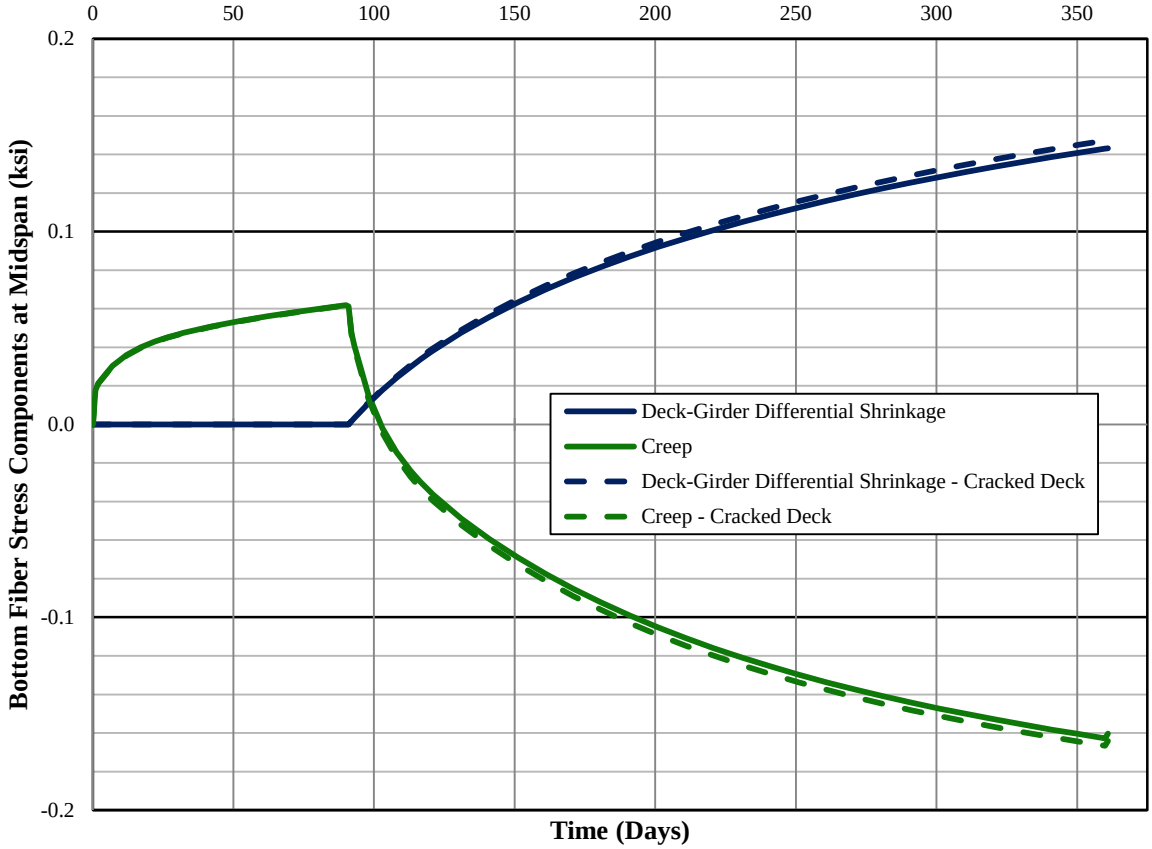

Figure 20. Bottom fiber stress due to creep and differential deck-girder shrinkage over time for no crack and cracked deck models

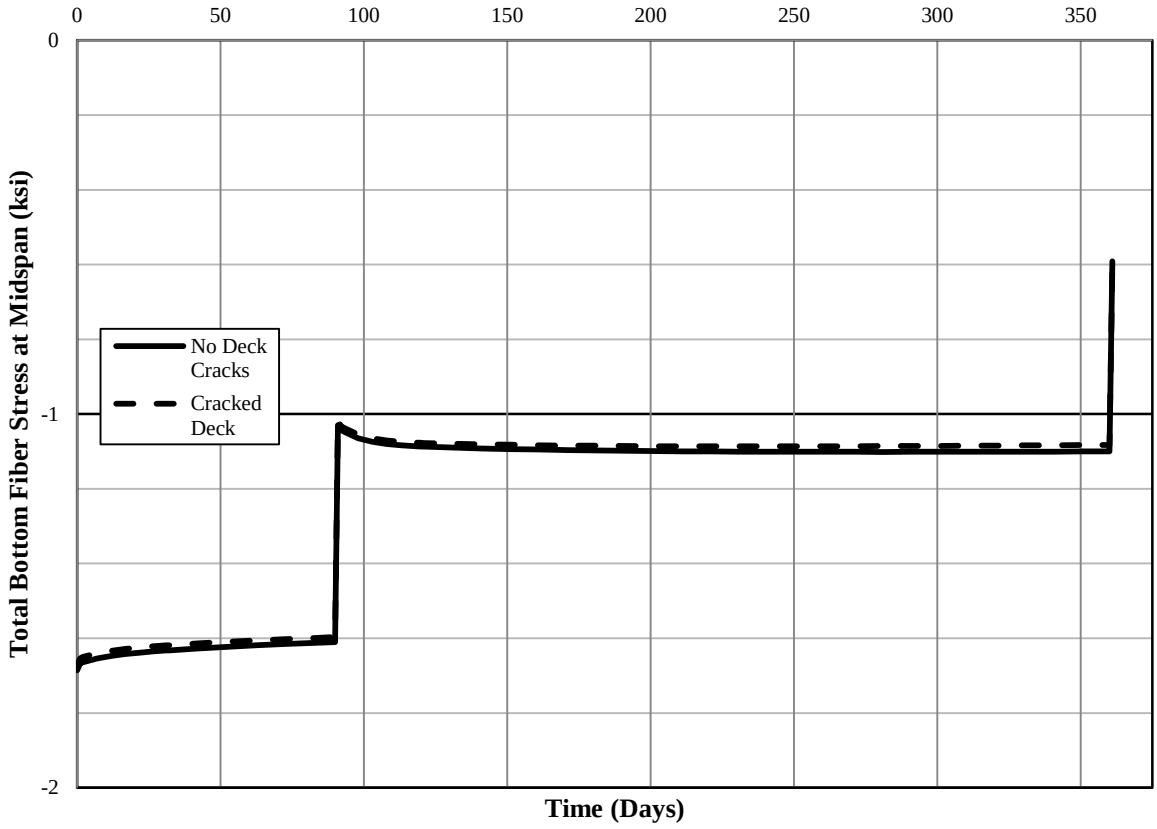

Figure 21. Total bottom fiber stress over time for no crack and cracked deck models

STRESS ANALYSIS WITH TRANSFORMED SECTION PROPERTIES

Flexural analysis of a member made of several materials involves creation of a fictitious homogeneous, or transformed, member. For this study, the prestressed girder and CIP deck are transformed into a homogenous material with modulus of elasticity, E_c.

The mechanics of transformed section properties were applied to verify the two and three dimensional FEMs. The flexural response of the prestressed concrete girder predicted by FEA was compared to hand calculations using transformed section properties. Concrete stresses due to prestress, self-weight, deck weight, and live load extracted from the three dimensional FEM matched manually calculated concrete stresses with negligible error. Stress output from the two dimensional model exhibited measureable error because the bar elements assigned to prestressing tendons do not displace concrete. A nearly perfect match is obtained when stresses are manually calculated based on a transformed section that includes the area of concrete displaced by steel. These results verify that the flexural response of the two and three dimensional models is consistent with fundamental mechanics using the appropriate transformed section properties. Refer to *Finite Element Model Verification* for more information on two dimensional modeling with bar elements.

CORRELATION OF PRESTRESS LOSSES AND BOTTOM FIBER STRESSES

Current AASHTO provisions instruct designers to monitor prestress losses at transfer, between transfer and deck placement, and between deck placement and final time. For pretensioned members, the total prestress loss is computed with AASHTO Equation 5.9.5.1-1. The formula is reproduced for reference in equation (6).

$$\Delta f_{pT} = \Delta f_{pES} + \Delta f_{pLT} \tag{6}$$

Long term prestress loss due to the time dependent effects of shrinkage, creep, and steel relaxation is defined in AASHTO Equation 5.9.5.4.1-1 and is reproduced in equation (7).

$$\Delta f_{pLT} = \left(\Delta f_{pSR} + \Delta f_{pCR} + \Delta f_{pR1}\right)_{id} + \left(\Delta f_{pSD} + \Delta f_{pCD} + \Delta f_{pR2} - \Delta f_{pSS}\right)_{df} \tag{7}$$

The design of prestressed concrete is typically controlled by service limit checks of stress in the extreme girder fibers. Prestress loss estimates are the means by which the concrete stresses are determined. The Specification provides guidance on calculating the losses, but does not offer instruction on how to use these values to determine concrete stresses.

Al-Omaishi et al. has published a method to compute bottom fiber concrete stresses associated with the AASHTO defined prestress losses.[7] The accuracy of this method and the correlation of prestress loss and extreme fiber concrete stress were examined using the two dimensional FEM. The results of this examination for losses between transfer and deck placement and between deck placement and final time are discussed below.

Time-Dependent Prestress Losses Between Transfer and Deck Placement

Correlation between concrete stress and prestress loss between transfer and deck placement (Time 0 to 90 days) was analyzed first. Changes in tendon stress due to beam shrinkage and creep and the associated concrete stresses were extracted from the FEA. Refer to the section *Component Isolation Procedure* for information on how stress and strain components were isolated. As stated previously, relaxation of the prestressing strands was not considered in this study.

Using the extracted prestress losses, concrete stresses were manually computed in accordance with methods published by Al-Omaishi, et al. based on net section properties and transformed section properties. The formula used to compute the change in concrete stress in bottom fibers due to loss between initial time and deck placement is reproduced in equation (8).[7]

$$\Delta f_{cb2} = \left(\Delta f_{pSR} + \Delta f_{pCR} + \Delta f_{pR1}\right)\left(\frac{A_{ps}}{A_g}\right)\left(1 + \frac{A_g e_{pg} y_b}{I_g}\right) \tag{8}$$

Top and bottom fiber stress calculations using net section properties matched the FEA output with negligible difference. Based on this result, girder concrete stresses due to pre-composite creep and shrinkage may be determined by applying the prestress loss to the net non-composite section (or the gross section with minimal error).

Time-Dependent Prestress Losses After Deck Placement

The investigation continued with the correlation of prestress losses after deck placement (Time 90 to 360 days) and related changes in concrete stresses. Again, steel relaxation was not considered, and deck shrinkage is addressed separately in this report.

Change in prestress due to beam shrinkage and creep and the associated concrete stresses were extracted from the FEA. The extracted losses were used to manually calculate concrete stresses in accordance with methods published by Al-Omaishi et al. based on net section properties and transformed section properties. The formula used to compute the change in bottom fiber stress due to loss between deck placement and final time is reproduced in equation (9).[7]

$$\Delta f_{cb4} = \left(\Delta f_{pSD} + \Delta f_{pCD} + \Delta f_{pR2}\right)\left(\frac{A_{ps}}{A_c}\right)\left(1 + \frac{A_c e_{pc} y_{bc}}{I_c}\right) \quad (9)$$

The first analysis of prestress losses after deck placement resulted in manually calculated concrete stresses that were considerably different from the FEA. Top and bottom fiber stresses differed by approximately 50% and 10%, respectively. Having confirmed the correlation of prestress losses and extreme fiber stresses between transfer and deck placement, the expectation was that the same relationship would be realized for the composite section. The most logical cause of the discrepancy was the presence of some behavior in the FEM that was not being considered in the hand calculations.

At the time of deck placement, both the deck concrete and the deck reinforcing are activated in the FEM. Similar to the prestressing tendons, deck reinforcing steel provides internal restraint against creep and shrinkage that is not considered when stresses are calculated using equation (9). Upon removing the mild steel deck reinforcing from the FEM, stresses matched well. Table 5 is a comparison of hand calculated and FEA predicted extreme fiber stresses. Hand calculations are based on equation (9) using net section properties

Table 5. Concrete Stresses due to Time Dependent Prestress Losses After Deck Placement

	(FEA) – (Hand Calculation)	
Location	With Deck Reinforcing	Without Deck Reinforcing
Top Fiber	-0.002798 ksi	0.000090 ksi
Bottom Fiber	0.001541 ksi	-0.000051 ksi

These results indicate that changes in girder concrete stress due to creep and shrinkage after deck placement may be determined by applying the prestress loss to the net composite section (or the gross section with minimal error). FEA results support the correlation between prestress loss and extreme fiber stresses proposed by Al-Omaishi et al..

NUMERICAL EXAMPLE

LUSAS FEM

Table 6 is a summary of values taken from the FEA output for comparison to hand calculations prepared in accordance with AASHTO provisions on prestress loss. Prestress losses and associated concrete stress changes are provided. A positive change in prestress represents a loss, and a positive concrete stress represents tension.

Table 6. FEA prestress loss and concrete stress output summary

	Δf_p	Deck-Top	Deck - Btm	Girder-Top	Girder-Bottom
Initial Prestressing and Self-weight					
Elastic shortening & Elastic gain	6.906			-0.822	-1.672
Shrinkage Before Deck Placement					
Stress change due to shrinkage	1.646			0.357	-0.336
Subtotal	8.552			-0.465	-2.008
Relaxation Before Deck Placement					
Stress change due to relaxation loss	0.000				
Subtotal	8.552			-0.465	-2.008
Creep Before Deck Placement					
Stress change due to creep	5.907			0.014	0.062
Subtotal	14.459			-0.451	-1.946
Deck Weight					
Stress change due to deck weight	-0.607			-0.586	0.579
Subtotal	13.852			-1.038	-1.368
Superimposed Dead Load					
Stress change due to SIDL	0.000				
Subtotal	13.852			-1.038	-1.368
Shrinkage After Deck Placement					
Stress change due to shrinkage	1.725	-0.002	0.002	0.003	0.019
Subtotal	15.577	-0.002	0.002	-1.035	-1.349
Relaxation After Deck Placement					
Stress change due to relaxation	0.000				
Subtotal	15.577	-0.002	0.002	-1.035	-1.349
Creep After Deck Placement					
Stress change due to creep	1.548	-0.002	-0.107	0.432	-0.229
Subtotal	17.124	-0.004	-0.105	-0.603	-1.578
Deck Shrinkage (Δf_{cdf})					
Stress change due to deck shrinkage	0.086	-0.017	0.103	-0.269	0.149
Subtotal	17.210	-0.021	-0.002	-0.872	-1.429
Live Load					
Stress change due to LL	-1.344	-0.203	-0.048	-0.061	0.475
Total	15.469	-0.224	-0.049	-1.288	-0.605

AASHTO

Table 7 is a summary of hand calculations prepared in accordance with AASHTO provisions on prestress loss supplemented by the published works of Al Omaishi et al.[2,7] A positive change in prestress represents a loss, and a positive concrete stress represents tension. The coefficients and shrinkage strains used in the computations were those extracted from Lusas.

Table 7. AASHTO prestress loss analysis summary

	Δf_p	Deck-Top	Girder-Top	Girder-Bottom
Initial Prestressing and Self-weight				
Elastic shortening & Elastic gain	6.901		-0.823	-1.691
Shrinkage Before Deck Placement				
K_{id}	0.943			
Stress change due to shrinkage	1.252		0.003	0.013
Subtotal	8.153		-0.820	-1.678
Relaxation Before Deck Placement				
Stress change due to relaxation loss	0.000		0.000	0.000
Subtotal	8.153		-0.820	-1.678
Creep Before Deck Placement				
Stress change due to creep	5.968		0.014	0.062
Subtotal	14.120		-0.806	-1.616
Deck Weight				
Stress change due to deck weight	-0.592		-0.587	0.581
Subtotal	13.528		-1.393	-1.035
Superimposed Dead Load				
Stress change due to SIDL	0.000		0.000	0.000
Subtotal	13.528		-1.393	-1.035
Shrinkage After Deck Placement				
K_{df}	0.936			
Stress change due to shrinkage	1.687	-0.002	0.003	0.018
Subtotal	15.215	-0.002	-1.390	-1.017
Relaxation After Deck Placement				
Stress change due to relaxation	0.000	0.000	0.000	0.000
Subtotal	15.215	-0.002	-1.390	-1.017
Creep After Deck Placement				
Δf_{cd}	-0.171			
Stress change due to creep	1.441	-0.002	0.002	0.015
Subtotal	16.656	-0.004	-1.387	-1.002
Deck Shrinkage				
Δf_{cdf}	-0.017			
Stress change due to deck shrinkage	0.132	0.383	-0.252	0.139
Subtotal	16.788	0.379	-1.640	-0.863
Live Load				
Stress change due to LL	-1.315	-0.244	-0.063	0.478
Total	15.472	0.135	-1.703	-0.385

Conclusion and Recommendations

The research presented in this paper uses finite element analysis (FEA) to study the behavior of a precast concrete bridge girder made composite with a CIP deck. A 30 foot long simply supported girder having a rectangular cross section and straight tendons was selected for the study.

Two timely issues related to precast concrete bridge design were investigated, and the following conclusions were drawn:

1. Differential deck shrinkage and its impact on the concrete stresses.
   Can deck shrinkage be modeled as an equivalent force?

A finite element study confirms that the shrinkage strain present in the deck over and above the girder shrinkage during the time period when the girder and deck are compositely bonded together can be modeled as an equivalent force equal to P_{deck}. The magnitude of P_{deck} (See Equation (2)) is computed using the difference between deck shrinkage and uniform beam shrinkage strains. This differs from the calculation of P_{deck} built into AASHTO[2] equation 5.9.5.4.3d-2, which uses total deck shrinkage. The proposed formula for P_{deck} provided in Equation (2) acknowledges that the equivalent force is generated by differential shrinkage between the deck and girder, not total deck shrinkage. This proposed revision accounts for the fact that the girder continues to shrink (albeit not as much as the deck) after the system is made composite.

   If so, how are girder and deck stresses calculated from that force?

Girder and deck stresses are computed by treating the force as an external load positioned on the deck centroid and acting on the transformed composite section. When using this method to compute deck stress, designers are reminded that both equilibrium and strain compatibility at the deck-girder interface must be considered.

   By how much is that force reduced when creep is considered?

When beam and deck creep are considered, the gross effect of differential deck shrinkage is reduced by approximately 40%, for the geometry and materials used in this study. Most of the reduction in top and bottom fiber girder stress is a result of beam creep. Additional research considering a variety of geometry and materials must be performed before any design recommendations can be proposed.

   By how much is that force reduced when deck cracking is considered?

The effects of differential shrinkage are not softened by the presence of cracks in the deck. Stress transfer from the deck to the beam, will continue with minimal reduction provided there is some connection between each volume of deck concrete and the girder and the deck remains uncracked between at least two adjacent transverse shear transfer locations. Any meaningful reduction in stress transfer is provided only by a severely cracked deck that

would have many other service-related issues. This conclusion is expected to apply to all beam and deck configurations.

2. The use of gross section properties and transformed section properties to compute concrete and steel stresses.
   How should concrete stresses be determined?
   How should prestress loss values be interpreted?

An examination of concrete stresses due to elastic effects and prestress losses was conducted. The results of the examination support the use of transformed section properties to determine the effects of prestress transfer on concrete, including elastic shortening.

Subsequent changes in concrete stress due to creep and shrinkage are determined by applying prestess loss values to the net section. Girder concrete stresses due to pre-composite creep and shrinkage are determined by applying the prestress loss to the net non-composite section (or the gross section with minimal error). Similarly, time dependent changes in girder concrete stress after deck placement are computed by applying the prestress loss to the net composite section (or the gross composite section with minimal error). These findings support the correlation between prestress loss and extreme fiber stresses published by Al-Omaish, et al. This conclusion is expected to apply to all beam and deck configurations.

Future Research

Over the course of this study, additional research needs were identified. Items requiring further research include creep superposition and creep softening of differential shrinkage effects.

The presence of a compressive creep stress component in the bottom fiber (see Figure 8) warrants further investigation of the defined component isolation procedure. Creep causes a loss of prestress that is represented with a tensile stress component in the bottom fiber. After deck placement, creep continues to cause prestress loss, but is also causing a reduction in tensile differential shrinkage effects. While this may explain the compressive creep stress component in the bottom fiber, one could interpret the graph as implying that creep helps to pre-compress the concrete if creep softening of differential shrinkage outweighs creep loss of prestress. Physically, creep does not act to pre-compress the concrete under any circumstances, thus suggesting that the nature of the creep models in the AASHTO and CEB specifications does not lend them to superposition of creep strains through situations of stress reversals.

Consider the graph shown in Figure 22. A time history of creep strain values from a prestressed column modeled in Lusas with properties very similar to the selected girder cross section is shown. Strain values are sampled from the prestressing centroid. The column is initially prestressed such that the stress in the concrete is approximately -1.45 ksi. At day 90, an axial tension force is applied to the column of a much smaller magnitude than the

prestressing force. The introduction of the tension forces causes the compressive stress in the concrete to be effectively reduced by 0.56 ksi, but the section is still in net compression. Although the section remains in net compression, the plot in Figure 22 indicates creep elongation of the column immediately following application of the small tension force. The creep trajectory from the large initial prestress force should be reduced by the tensile force applied at day 90, but the plot should recover quickly and start moving towards a net shortening strain. The creep strains shown do not represent such behavior; rather the plot maintains a net creep elongation through the end of the analysis. Future research is needed to assess the effects of creep due to a series of sustained loads.

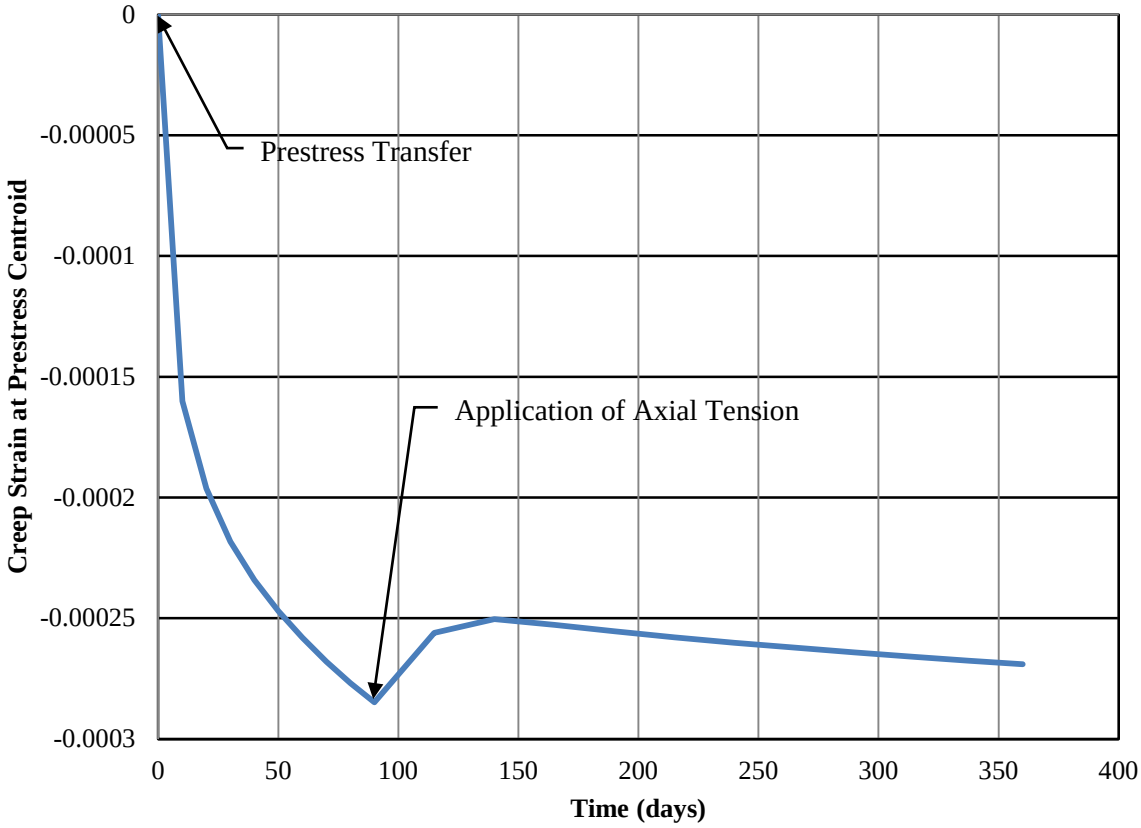

Figure 22. Creep Superposition Check

Further research is also needed to formulate recommendations and conclusions on creep softening. The results presented in the *Deck Shrinkage* section of this report state that the portion of net effect of differential shrinkage, which includes beam and deck creep, is approximately 60% of the gross effect, for the geometry and materials used in this model. Considering that concrete creep is a function of time, applied load, material properties and geometry, this numerical value for creep softening cannot be extended to other beam-deck configurations. Future research in the form of a parametric study that quantifies creep softening for numerous combinations of geometry, material, and span configuration is needed.

REFERENCES

1. Tadros, Al-Omaishi, Seguirant, and Gallt. 2003. “Prestress Losses in Pretensioned High-Strength Concrete Bridge Girders,”National Cooperative Highway Research Program Report 496. Washington, DC: Transportation Research Board, National Academy of Sciences.

2. American Association of State Highway and Transportation Officials (AASHTO). (2010). “AASHTO LRFD Bridge Design Specifications.” Fifth Edition, Washington, DC.

3. Swartz, B. D., Schokker, A. J., and Scanlon, A., Simplification of Prestress Loss Provisions for the AASHTO-LRFD Bridge Design Specifications, SN3123, Portland Cement Association, Skokie, Illinois, USA, 2010, 190 pages.

4. Lusas, “Element Reference Manual.” Lusas Version 14.7: Issue 1, United Kingdom, 2011, pp. 54-58, 116-121, 204-210.

5. Lusas, “Solver Reference Manual.” Lusas Version 14.7: Issue 1, United Kingdom, 2011, pp. 102-105, 113-115, 130-132, 142-153, 269-284.

6. Comité Euro-International du Béton, “CEB-FIP Model Code 1990: Design Code.” FIB - Féd. Int. du Béton, 1993.

7. Cartier, T. R. and Swartz, B. D., A Finite Element Study of Deck Shrinkage and Stress Analysis in Composite Bridge Girder Systems, University of Hartford, West Hartford, CT, 2012.

8. Al-Omaishi, Tadros, and Seguirant, “Estimating Prestress Loss in Pretensioned, High-Strength Concrete Member,” PCI Journal, Fall 2009, pp. 132-159.

DEFINITIONS

e_d	=	eccentricity of the deck with respect to the centroid of the transformed composite section
ε_{bdf}	=	shrinkage strain of beam between deck placement and final time
ε_{ddf}	=	shrinkage strain of deck between placement and final time
$\varepsilon_{ddf} - \varepsilon_{bdf}$	=	differential shrinkage between the cast-in-place deck and the precast girder
Δf_{pCD}	=	prestress loss due to creep of girder concrete between time of deck placement and final time (ksi)
Δf_{pCR}	= deck	prestress loss due to creep of girder concrete between transfer and placement (ksi)
Δf_{pR1}	=	prestress loss due to relaxation of prestressing strands between time of transfer and deck placement (ksi)
Δf_{pR2}	=	prestress loss due to relaxation of prestressing strands between time of deck placement and final time (ksi)
Δf_{pSD}	=	prestress loss due to shrinkage of girder concrete between time of deck placement and final time (ksi)
Δf_{pSR}	=	prestress loss due to shrinkage of girder concrete between transfer and deck placement (ksi)
Δf_{pSS}	=	prestress gain due to shrinkage of deck in composite section (ksi)
$\left(\Delta f_{pSR} + \Delta f_{pCR} + \Delta f_{pR1}\right)_{id}$	=	sum of time-dependent prestress losses between transfer and deck placement (ksi)
$\left(\Delta f_{pSD} + \Delta f_{pCD} + \Delta f_{pR2} - \Delta f_{pSS}\right)_{df}$	=	sum of time-dependent prestress losses after deck placement (ksi)
y_{bc}	=	eccentricity of bottom fibers with respect to the centroid of the transformed composite section
y_{dc}	=	eccentricity of the extreme bottom deck fiber with respect to the transformed composite centroid
A_d	=	net area of the deck concrete
A_{tr_c}	=	area of transformed composite section
A_{tr_nc}	=	area of transformed non composite section
E_{cd}	=	modulus of elasticity of deck concrete (ksi)
I_{tr_c}	=	moment of inertia of the transformed composite section
P_{deck}	=	effective force due to deck shrinkage applied to the composite section at the centroid of the deck.